

# Plastic Behavior Laws of Aluminum Aerospace Alloys: Experimental and Numerical Study

Olfa Daghfes\*, Amna Znaidi\* and Rachid Nasri\*

## ABSTRACT

The aim of this work is to study the anisotropic behavior of an aluminum alloy using a behavior model. The identification of this model requires an appropriate set of experimental database. Thus, the simple tensile tests (in and off axis) are carried in three loading directions relative to the rolling direction. This database consists of various curves of hardening for tensile tests interpreted as homogeneous and their Lankford coefficients. In order to further refine the experimental part of this work, microstructural observations were conducted through Transmission Electronic Microscopy to show interactions between the precipitates and dislocations in studied material. The experimental results obtained from uniaxial tensile tests are first described in order to show anisotropic behavior. Subsequently, an identification strategy will be implemented with regard to several hypotheses using a non-quadratic anisotropic yield function and isotropic hardening laws. The results show a good agreement between the theoretical results and experimental data.

## INTRODUCTION

Pure aluminum presents little of interests because its mechanical characteristics are poor. In contrast, the aluminum alloy used with addition elements is intended largely to improve its mechanical characteristics. Combined with lightness of the structure, they occupy a very important place in transport sector especially in the aerospace and the automobile (Williams, 2003). The aluminum alloys of the 2000 series (Cu is the main addition element) are essentially aeronautics alloys. They have a low density and high mechanical properties which allow their use as structural materials. The mechanical strength of these alloys is increased by structural hardening phenomenon (Dursun and Soutis, 2014). Alfred Wilms' study (Wilm, 1911) showed that an Al-Cu alloy hardened during aging at room

temperature after quenching. Today, hardening by precipitation has become a common practice in metallurgy. A significant number of studies have been carried out in the case of aluminum alloys of the 2000 series to characterize the precipitation. Nie and Muddle (2001) studied the hardening mechanisms of precipitates in the form of platelets. Their study reveals that the precipitates are sheared by the dislocations regardless of the duration of tempering. It is unlikely that there is transition between shearing and bypassing of the precipitates by dislocations. Majimel et al. (2004) analyzed the role of thermal activation on dislocation mechanisms. They have shown that thermal activation associated to a decrease of the precipitate density, softens the material and seems to facilitate bypassing of precipitates and the production of mobile dislocations. Li et al. (2008) find that the decrease in resistance observed after tempering is due to the coalescence of the hardening precipitates and they do not envisage a shear-to-bypass transition.

Sheet metals or plates are obtained by hot and cold rolling which creates plastic anisotropy. The plastic behavior is well described by a load surface which evolves during the plastic deformation for different tests. Mechanical properties and plastic behavior that give rise from the processing of aluminum alloy sheet especially cold rolling has been reported by many authors from several different mechanical experiments. These experiments include tensile tests (Barlat et al, 1991), static and dynamic compression (Ryzińska and Gieleta, 2016) pure shear tests (Gilmour et al, 2001) and combined loading tests (Lesuer, 2000) on specimens with several geometries (bar, plate, sheet).

The wide variety of real materials is reflected by the existence of many criteria and evolution laws in elastoplasticity (Dogui, 1989). Thus, the first anisotropic yield criterion was proposed by Hill (Hill, 1948) for materials, such as rolled sheets. The yield function of Hill has been widely used because it is quite suitable for steels and it is rather easy to implement (Slota and Diser, 2016). However, Bron (2004) has been found that Hill's criterion is inaccurate for aluminum alloys.

An important extension of this yield function to anisotropic materials was done by Barlat et al (1991). Their study of a thin aluminum sheet showed anisotropic plasticity response that led to a proposed six component yield function to model the anisotropy.

*Paper Received December, 2017. Revised January, 2018, Accepted January, 2018. Author for Correspondence: olfa daghfes.*

*\* Doctor in mechanics University of Tunis El Manar, National School of Engineers of Tunis, LR-MAI-ENIT BP37, 1002, Tunisie*

Several hardening laws are used to describe the isotropic hardening such as Hollomon law, Swift law, Ludwick law and Voce law (Voce, 1948; Bron, 2004).

This work consists of three parts. In first part, the main purpose is to carry out experimental uniaxial tensile tests on aluminum alloy in three directions relative to the rolling direction. The database corresponds to various curves of hardening for tensile tests interpreted as homogeneous and their Lankford coefficients. In the second part, in order to examine the behavior of 2024 aluminum alloy, the mechanical properties and the anisotropic behavior are investigated from the experimental database. A series of visualization on the TEM allowed us to see the microstructural state, its chemical composition and the behavior of the dislocations when the material is subjected to solicitations. The anisotropic behavior is identified using a proposed strategy with a Simplex method and followed by a validation from the Lankford coefficient. Furthermore, it is used to represent the evolution of anisotropy in terms of yield stress of this material. In the last part, the evolution of the load surface is conducted for several tests.

### EXPERIMENTAL PROCEDURE

#### Test Materials

The 2024 aluminum alloy with structural hardening was used. This alloy is a thin rolled sheet obtained by hot rolling whose thickness is 1.5 mm. Using Scanning Electron Microscopy (SEM) associated with X-ray Dispersive Energy Spectroscopy (EDX) in CETIME, the chemical composition of the studied alloy is shown in Table1. To obtain the required mechanical properties, this material has undergone different structural hardening treatments. In this study, the used commercial alloy in state T375 is subsequently referred to 2024 -T3. The heat treatment is carried out in an electric furnace with uniform temperature. The specimens of Al 2024 have suffered a heating to the temperature of dissolution  $495 \pm 5$  followed by an isothermal hold for homogenizing the structure. This thermal treatment is completed by a quenching in water at room temperature.

Table 2 presents the heat treatment applied to 2024 alloy.

Table 1. Chemical compositions of 2024-T3

Si	Cu	Mn	Mg	Cr	Zn	Ti	Fe	Al
0.5	4.9	0.9	1.8	0.1	0.25	0.15	0.5	remainder

Table 2. Heat treatment applied to 2024-T3

Solutionizing	Quenching	pre-stretching	Maturation
495°C ( ± 5°C)	Water < 40°C	2%	Room T° >4 days

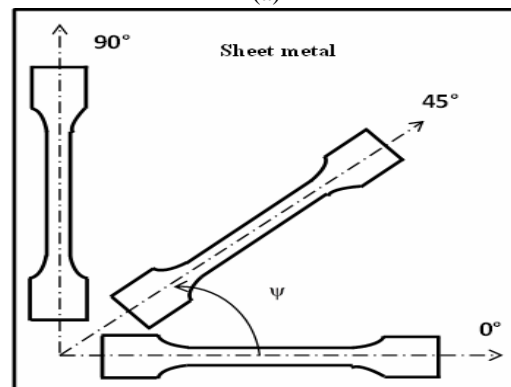
#### Dimensions and form of the test specimens

The uniaxial tensile test is ensured by a specific geometry defined by the standard NF A 03-151 (AFNOR, 1971). The latter standard specifies the forms and dimensions of the specimen as follows in Figure 1. Thickness of metal sheet is 1.5mm.

In order to avoid hardening and any residual stresses, the metal sheet was cut by laser (Figure 2) according to the standard NF 10002 (Barralis and Maeder, 1995).



(a)



(b)

Fig. 2(a) Direction of cutting: RD (0°), TD (90°) and (45°) respecting to the rolling direction (b) aluminum alloy sheets during the cutting phase by laser

x:Rolling direction, y: direction perpendicular from the rolling direction in the plane of the sheet, z : normal direction to plane of the sheet.

The specimens are cut in three orthogonal directions relative to the rolling direction in the plane of the sheet. These directions are defined as: rolling direction 0° (RD), transverse direction 90° (TD) and 45° direction from the rolling direction (see Fig.2 (b)). The angle between the loading direction and the rolling direction will be noted subsequently  $\psi$ .

Three samples in each loading direction were performed in testing machine to verify repeatability.

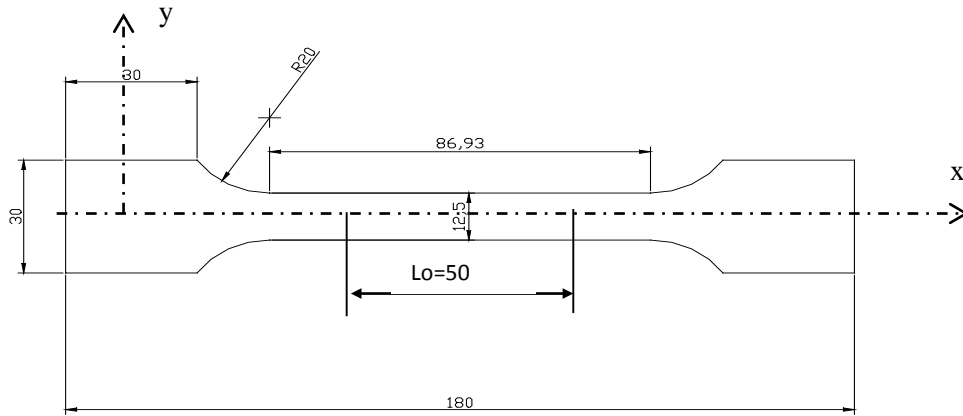


Fig.1 Forms and dimensions of tensile specimen, the useful area ( $L_0=50\text{mm}$ ,  $b_0 = 12.5\text{mm}$ )

### Experimental set:

Uni-axial tensile tests are being conducted on a hydraulic press (Figure 3 (a)) with a load capacity of 30 tonnes (accuracy on the load and the displacement is 0.5%). The data acquisition is done on computer via an acquisition chain. The longitudinal and transversal deformations were measured by an extensometer with 0.1% precision, respectively (Figure 3(b)). The crosshead speed equal to 10mm/min is maintained constant through the test.



(c)

Fig. 3. Experimental equipment used to perform the tests (a) Tensile test machine (b) Extensometer [LGM] (c) TECNAI F20 (SACTEM-TOULOUSE)

The crosshead speed equal to 10mm/min is maintained constant through the test.

In which the machine coupled to a computer via software, the load (F), the longitudinal displacement and transversal displacement are measured.

We can therefore get axial  $\epsilon_{xx}$ , transverse  $\epsilon_{yy}$ , normal  $\epsilon_{zz}$  strains and the instantaneous stress from the following formulas:

$$\epsilon_{xx} = \text{Log}(L/L_0); \epsilon_{yy} = \text{Log}(b/b_0) \quad (1)$$

$$\epsilon_{zz} = \text{Log}(e/e_0); \sigma = F/S = (F/S_0)e^{-(\epsilon_{yy} + \epsilon_{zz})}$$

Where  $L_0$  and  $L$ ,  $b_0$  and  $b$ ,  $e_0$  and  $e$  are initial and current values of length, width and thickness of specimen respectively.

### Microstructure characterisation

Microstructural characterization studies were conducted on specimens of 2024 aluminum alloy



(a)



(b)

before and after the tensile test to investigate the dislocation, the precipitation and the interaction between them. The samples about 3mm diameter and 50 μm thick were obtained and were polished with abrasive papers of grades 120, 800 and 1200 and attacked with the reagent of killer.

They were examined using a JEOL 2010 transmission electron microscope (Figure 3.c) from the TEMSCAN in Toulouse.

### IDENTIFICATION METHOD

In this section, we are interested in plastic orthotropic behavior; the material is treated as incompressible with negligible elastic deformations. Models are formulated for standard generalized materials with an isotropic hardening described by an internal hardening variable denoted by  $\varepsilon^p$ , an evolution law and an equivalent deformation material is initially orthotropic remains orthotropic (Znaidi et al, 2016). In order to simplify the identification method, the tensile test conducted in the rolling plane is considered homogenous and the hardening is isotropic.

The behavior model is then written as follows:

#### Yield criterion

The representation of a yield function  $f$  in the principal stress space constitutes the load surface, the interior of this surface representing the elastic domain. It must be convex and closed. Formally, it is written as:

$$f(q, \varepsilon^p) = \sigma_{eq}(q) - \sigma_y(\varepsilon^p) \leq 0 \quad (2)$$

$\sigma_{eq}$  : Equivalent stress. Its expression varies according to the authors and their approaches In this work, the Barlat criterion (Barlat et al, 1991) is used:

$$\sigma_{eq}(\mathbf{q}) = \left( |q_1 - q_2|^m + |q_2 - q_3|^m + |q_1 - q_3|^m \right)^{1/m} \quad (3)$$

where  $q_{k=1,2,3}$  are the eigenvalues of a modified stress deviator tensor  $\mathbf{q}$  defined as follows:

$$\mathbf{q} = \mathbf{A} : \boldsymbol{\sigma}^D \quad (4)$$

The fourth order tensor  $\mathbf{A}$  carries the anisotropy by 6 coefficients  $c_1, c_2, c_3, c_4, c_5, c_6$ .  $\boldsymbol{\sigma}^D$  : the stress deviator tensor.

$\sigma_y(\varepsilon^p)$  represents the scalar variable of isotropic hardening.

$\varepsilon^p$  is the equivalent plastic strain.

#### Hardening law

The hardening laws and variables describe the evolution of response material which is subjected to a charge.

The main isotropic behavior laws used for aluminum alloys are:

Hollomon law:

$$\sigma_y(\varepsilon^p) = K(\varepsilon^p)^n \quad (5)$$

Voce law:

$$\sigma_y(\varepsilon^p) = \sigma_s + (1 - \alpha \exp(\beta \varepsilon^p)) \quad (6)$$

This law introduces a hardening saturation  $\sigma_s$ ,  $\alpha$  and  $\beta$  describe the non-linear part of the curve during the onset of plasticity where  $0 < \alpha < 1$  and  $\beta < 0$ .

#### Evolution law

The direction of the plastic strain rate  $\dot{\varepsilon}^p$  is perpendicular to the yield surface and is given by:

$$\dot{\varepsilon}^p = \dot{\lambda} \frac{\partial f}{\partial \boldsymbol{\sigma}^D} \quad (7)$$

where  $\dot{\lambda}$  is the plastic multiplier determined from the condition of volume consistency (zero plastic volume change):

$$\dot{\varepsilon}_{xx} + \dot{\varepsilon}_{yy} + \dot{\varepsilon}_{zz} = 0 \quad (8)$$

#### Anisotropy coefficient

In the characterization of thin sheets, the plastic anisotropy with different directions is frequently measured by the Lankford coefficient  $r_\psi$  that is given by the following expression:

$$r_\psi = \dot{\varepsilon}_{yy} / \dot{\varepsilon}_{zz} \quad (9)$$

where  $\dot{\varepsilon}_{yy}$  and  $\dot{\varepsilon}_{zz}$  are the plastic strain rates in-plane and through the thickness, respectively.

In the case of orthotropy  $r_\psi$  varies depending on the off axis angle  $\psi$ . It is usually determined for three different directions of loading in-plane ( $r_{0^\circ}, r_{45^\circ}$  and  $r_{90^\circ}$  to the rolling direction).

In order to simplify the identification method, the tensile test conducted in the rolling plane is considered homogenous and the hardening is isotropic.

## RESULTS AND DISCUSSION

### Experimental data

Experimental database for 2024 aluminum alloy contains three experimental tensile curves (Figure 4) and their Lankford coefficients  $r_0, r_{45}$  and  $r_{90}$  (Table 3).

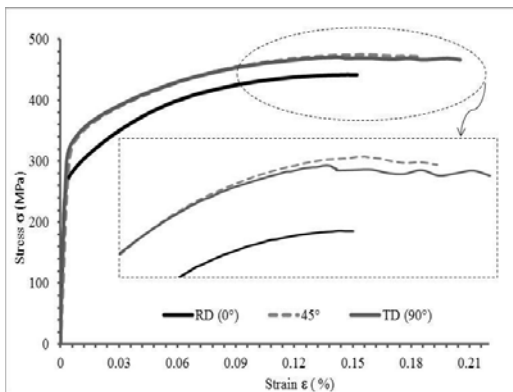


Fig. 4 Experimental stress-strain curves obtained at 0°, 45°, and 90° to the RD for 2024-T3

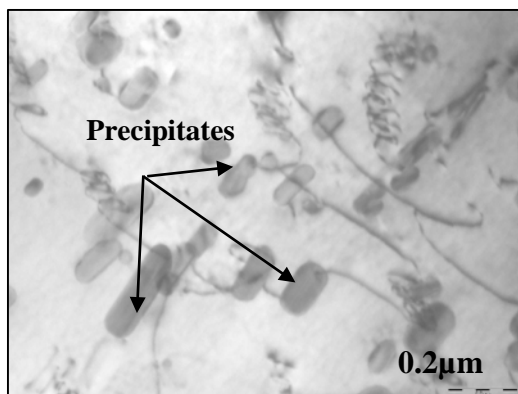
For Fig. 4 shows similar yield strength and ultimate tensile strength in 45° and 90° directions until 18 % in strain. However at the rolling direction 00°, they are both weaker. The slope of strain hardening sensibly remains the same for the three loading directions.

In heterogeneous plastic deformations (by zooming the necking zone) the hardening is replaced by a softening followed by a slight hardening. This latter is more noticeable in 90° direction.

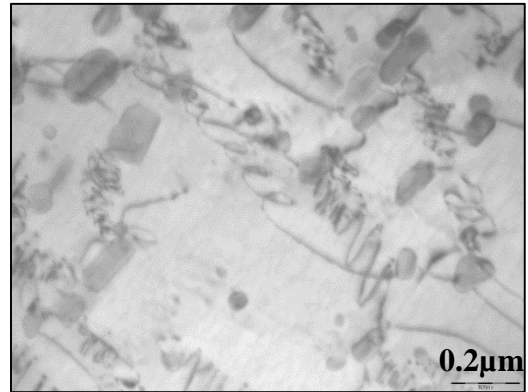
Their mechanical characteristics in terms of the young's modulus  $E$ , the Poisson's ratio  $\nu$  and the experimental Lankford coefficients determined from tensile tests are summarized in Table 3.

Table 3. Mechanical characteristics of 2024-T3 alloy

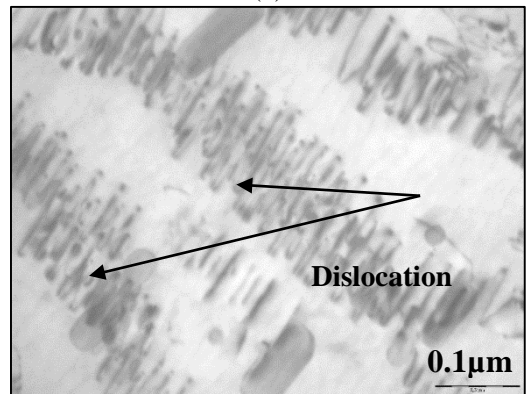
E(GPa)	$\nu$	$r_0$	$r_{45}$	$r_{90}$
73	0,33	0,741	0,972	0,981



(a)

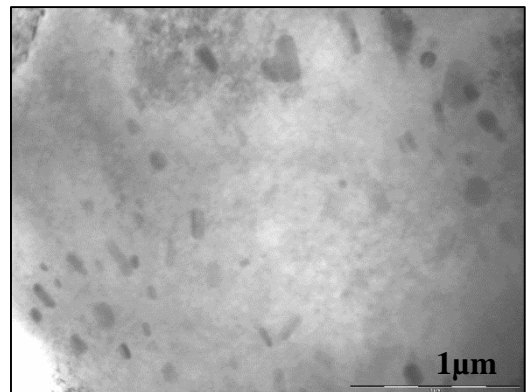


(b)

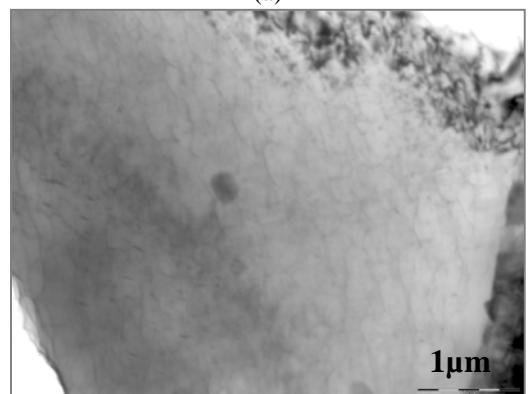


(c)

Fig.5 Microstructure of dislocations in non-deformed Heat treated specimen (TEM)



(a)



(b)

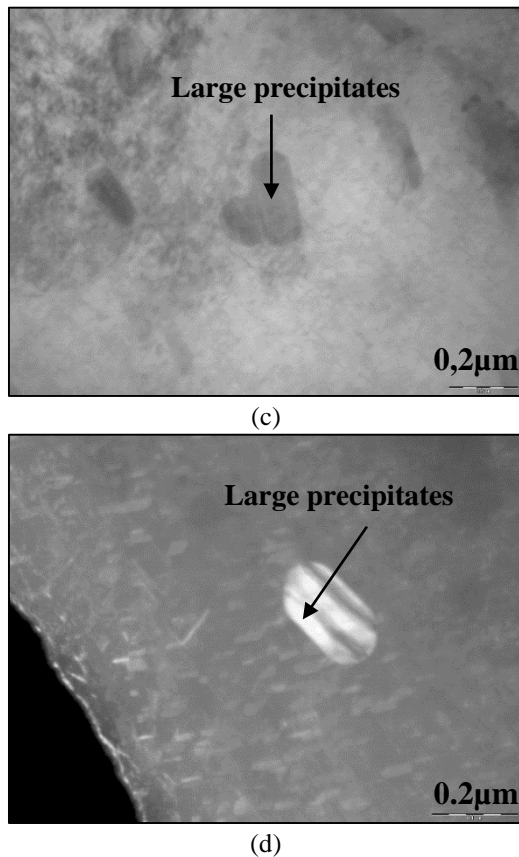


Fig.6 Microstructures of dislocations in deformed specimen (TEM)

During the forming process, the sheets are hot rolled then cold rolled before being annealed. The rolling involves the alignment of the intermetallics and the dispersoids, as well as the elongation of the grains.

Considering the chemical composition of studied material, three types of precipitates are present. The largest are intermetallics, aligned along the direction of rolling. They have a detrimental effect on toughness. The second type (dispersoids) has an average size which is in the form of stick. Finally, the third type is a fine precipitate which is in the form of inclined platelets. Hot deformation has other consequences in terms of the microstructure and more particularly as regards the density of dislocations. Indeed, the structure is heterogeneous with grains containing many dislocations and others very few (Figure 5).

Knowing that it is a heat treated material, the presence of precipitates and dislocations is very important. The 2024 alloy in the T351 state is stressed (pre-stretched) between tempering and maturation, which introduces dislocations (Fig.5). The mechanical properties of the alloys in this series are increased due to the presence of fine precipitates of a second phase. This type of alloy is

thus constituted by hardening precipitates such as (Al<sub>2</sub>Cu).

The presence of precipitation and dislocations is likely to harden the material. This is due to the structural hardening by precipitation applied to studied material. This phenomenon is explained by the interaction between the dislocations and the precipitates. As the fine particules are harder than the matrix of the material the dislocations cannot penetrate the precipitates. So they are forced to by-pass them (see Fig. 5). This latter create a softening of the material as shown in Fig. 5 particularly in TD direction.

Whereas once plasticity is reached these dislocations disappear and remain only the precipitates (Figure 6(a)). In Fig. 6(b), the small precipitates are of size 10 nanometers and the large ones of size 20 nanometers which has detrimental effect for the mechanical properties (Fig. 6(c)).

Fig. 6 shows the deformed states. It reveals entanglements of the dislocations without the slightest reorganization in hardening cells. This suggests the presence of slippage mechanisms at room temperature (without temperature effect) at very high displacement rates.

**Identification of hardening curves**

Material parameters for the HOLLomon (Eq(5)) and VOCE (Eq(6)) laws are fitted using experimental tensile curves at 00°, 45° and 90° from the rolling direction RD. The obtained sets of parameters are shown in Table 4, for the two laws.

Table 4. Identified parameters of two laws

$\psi$ (°)	HOLLomon		VOCE		
	k	n	$\sigma_y$	$\alpha$	$\beta$
00	619.15	0.161	451.49	0.43	-21.68
45	608.56	0.126	482.25	0.35	-19.63
90	598.31	0.119	475.46	0.35	-21.75

From the identified parameters of two laws, it is seen that 2024-T3 alloy has sufficient consolidation capacity which proves good behavior in simple tensile test.

Furthermore, it appears that 2024 alloy has the maximum strain hardening exponent along the rolling direction and minimum value along transverse direction.

Figure 7 presents the identification curves by the HOLLomon and the VOCE laws compared to the tensile experimental curves obtained in the three directions relative to the rolling direction.

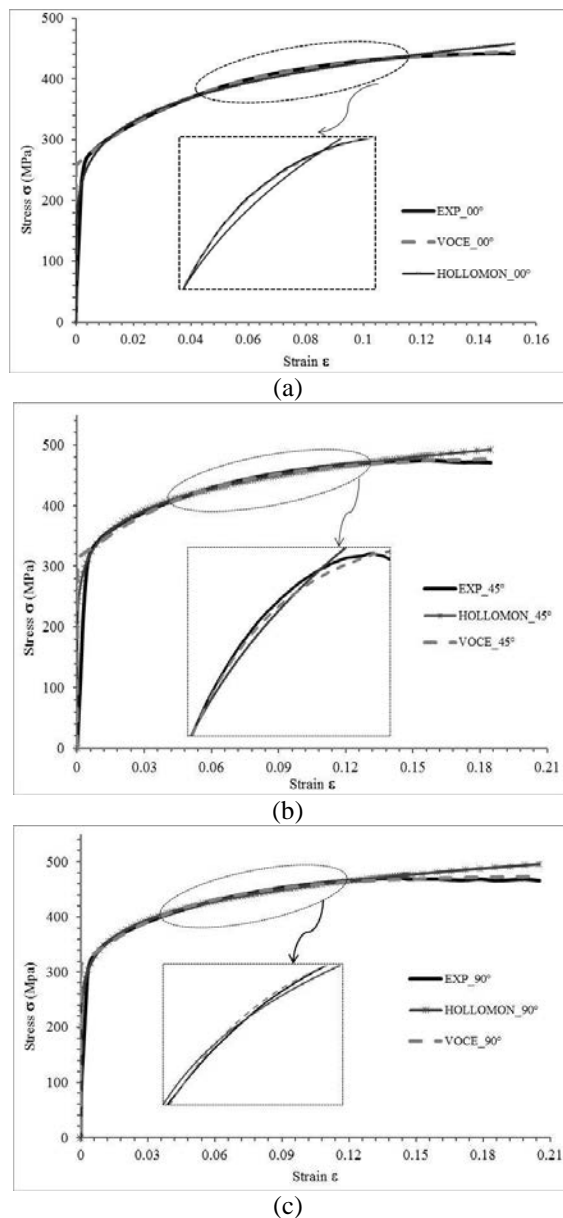


Fig. 7 Identification of the hardening curve: (a)  $\psi = 00^\circ$  (b)  $\psi = 45^\circ$  (c)  $\psi = 90^\circ$

Fig.7 (a), (b) and (c) show a net adjustment between the theoretical and experimental results. A significant difference in result between the two laws is noticeable in the two areas. By zooming the first area, it is seen that the VOCE law is better than the HOLLONOMON law.

This is explained by the quality of its phenomenological formula (Eq6) related to dislocations distributions. It predicts both hardening and softening effects as shown in two selected areas.

By convention, the voce hardening law is selected subsequently to identify anisotropy behavior relating to this material.

### Identification of anisotropic plasticity model

Using the plastic Barlat criterion, the voce hardening law and respecting the assumptions, the identification is equivalent to choosing the model parameters using the simplex method by minimizing the quadratic error between experimental and numerical results. By considering plane stress condition, the anisotropy parameters of the Barlat criterion are reduced to 4 ( $c_1, c_2, c_3, c_4$ ). Identified anisotropy parameters and shape coefficient  $m$  related to Barlat criterion are presented in Table 5.

Table 5. Identified anisotropy parameters and shape coefficient  $m$

$c_1$	$c_2$	$c_3$	$c_4$	$m$
0.3078	0.306	0.3078	0.91	7.672

### Validation of identification strategy

As the experimental tensile curves are used to identify the parameters of the behavior model, the Lankford coefficients are used to validate our identification strategy.

The evolution of Lankford coefficient based on off-axis angles is shown in Figure 8.

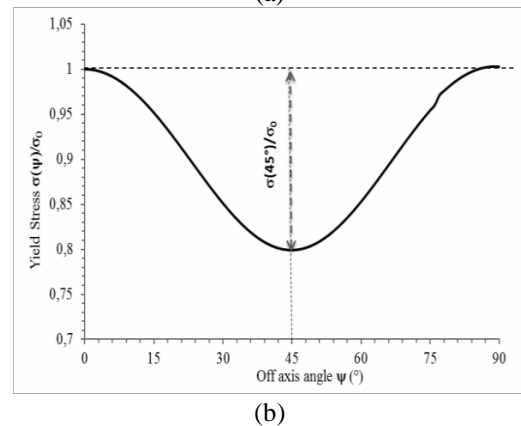
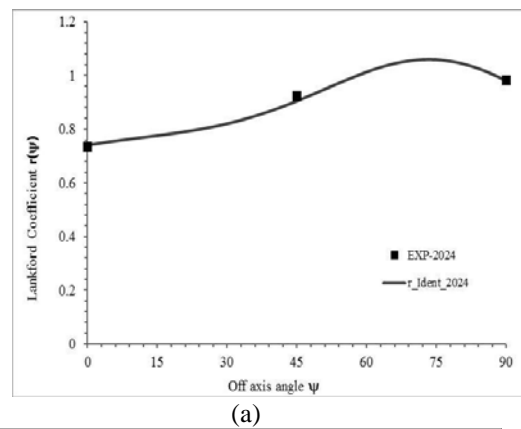


Fig.8: Evolution of (a) Lankford coefficient and (b) yield stress anisotropy based  $\psi$

A good agreement has been found between experimental and predicted Lankford coefficients with respect to the rolling direction. Thus, the behavior model describes very well the plastic behavior of this alloy. The evolution of normalized yield stress based on off-axis angles is shown in Fig. 8(b). The evolution of anisotropy of 2024-T3 is more pronounced in 45° direction from the rolling direction. Therefore the 2024-T3 is more suitable for forming process for the manufacture of the aerospace parts. This confirms the evolution of load surfaces related to this alloy for different tests.

**Evolution of the yield surface in deviatoric plane**

$$(\bar{x}_2, \bar{x}_3)$$

Using the identified anisotropic coefficients (Table 5), the behavior model allows to represent the shape of the yield surfaces on each test (simple tensile, simple shear, plane tensile) in the deviatoric plane (Daghfas et al, 2015; Znaidi et al, 2016; Daghfas et al, 2019).

Figure 9 shows the evolution of the yield surfaces on different tests.

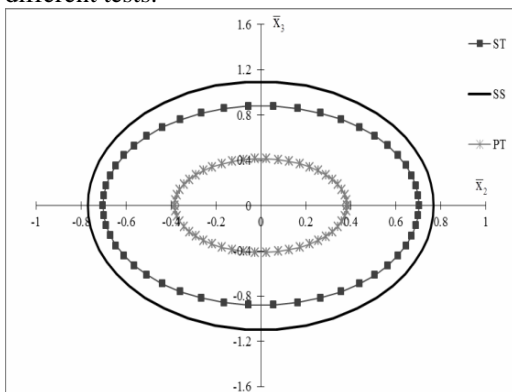


Fig. 9: Evolution of the yield surface in deviatoric plane  $(\bar{x}_2, \bar{x}_3)$  of simple tensile ST, simple shear

SS and Plane tensile PT

**Finite element simulation**

A similar tensile specimen as the experimental one is used for the numerical simulation and its finite element mesh is presented in Figure 10.

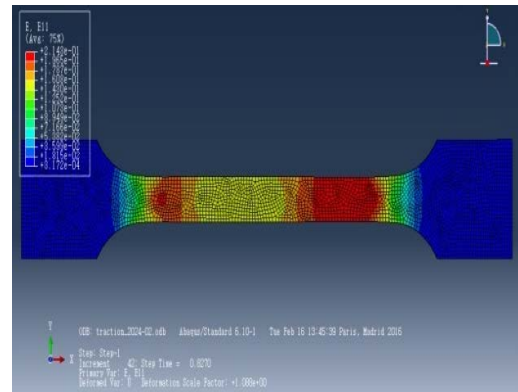
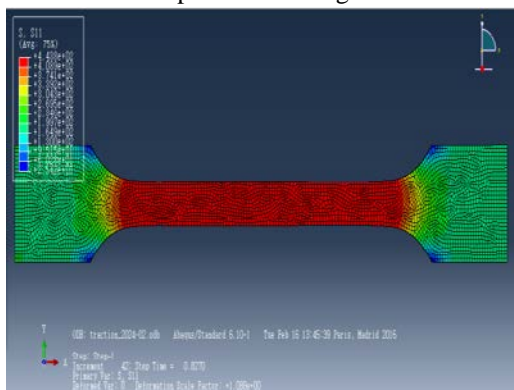


Fig. 10 Finite Element meshes for the tensile specimen

The voce law describing an isotropic hardening are identified from the experimental tensile test at 0° and are defined by:  $R=30I+250[1- \exp(-18\lambda)]$ .

A numerical simulation of a tensile test along the rolling direction using a Voce law is shown in Figure 11.

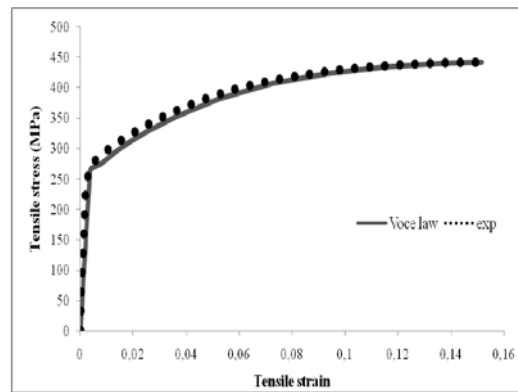


Fig.11: Numerical simulation of a tensile test

**CONCLUSIONS**

Since the commercial 2024-T3 alloy is used for the manufacture of the aerospace parts, we investigated their plastic behavior and the evolution of anisotropy.

In this study, off-axis tensile tests applied to this material are launched. The experimental response has allowed to investigate the mechanical properties and to identify plastic behavior model using a proposed identification strategy. A micrographic study allowed us to observe the movement of the dislocations and their interaction with the precipitates which explains the phenomena of hardening and softening of studied material. The calculation results of proposed strategy were in good agreement with the experiment results, because its yield function and its hardening law are suitable for aluminum alloys.

The influence of the off-axis angle on anisotropy is studied.

It is deduced that the best shaping in the design of the aerospace parts is realized using the 2024 alloy sheet in the loading direction at  $\psi = 45^\circ$  from rolling direction.

In order to obtain a complete description of plastic anisotropy in large deformations, an experimental simple and cyclic shear tests will be conducted. The identification strategy can be improved by introducing the kinematic hardening models.

## ACKNOWLEDGMENT

The authors gratefully acknowledge the members of the Mechanical Engineering Laboratory at National Engineering School of Monastir Tunisia [MEL] and TEMSCAN-CEMES of the Toulouse University for the TEM observations.

## REFERENCES

Barlat F., Lege D. J., Brem J.C., “A Six-Component Yield Function for Anisotropic Materials”. *International Journal of Plasticity*, 7, 693-712 (1991).

Barralis J., Maeder G., “Precise metallurgy – Elaboration, Structures, Properties”, (French) Normalisation AFNOR – NATHAN, (1995).

Bron F., “Ductile tearing thin 2024 aluminum alloy sheets for aeronautical application”, PhD thesis, Nationale school of Mines of Paris, (2004).

Daghfas O., Znaidi A., Gahbiche A., Nasri R., “Identification of the anisotropic behavior of an aluminum alloy subjected to simple and cyclic shear tests”, *Proc IMechE Part C: J Mechanical Engineering Science*, Vol. 233(3) 911–927, (2019).

Dogui A., “Anisotropic plasticity in large deformation”, PhD thesis of sciences, University Claude Bernard-Lyon I, (1989).

Dursun T., Soutis C., “Recent developments in advanced aircraft aluminium alloys”, *Materials and Design*, 56, 862–871, (2014).

French standard NF A 03-151, “Traction test”, French Association for Standardization (AFNOR), (1991).

Gilmour K. R., Leacock A. G., Ashbridge M.T.J., “The Determination of the In-Plane Shear Characteristics of Aluminum Alloys”, *Journal of Testing and Evaluation*, 29, 131-13, (2001).

Hill R., “A Theory of the Yielding and Plastic Flow of Anisotropic Metals”, *Mathematical and Physical Sciences*, 193, 281-297, (1948).

Lesuer D. R., “Experimental Investigations of Material Models for Ti-6Al-4V Titanium and 2024-T3 Aluminum”, Report No. DOT/FAA/AR-

00/25, (2000).

Li H., Tang Y., Zeng Z., Zheng Z., Zheng F., “Effect of ageing time on strength and microstructures of an Al-Cu-Li-Zn-Mg-Mn-Zr alloy”. *Materials Science and Engineering : A*, 498:314– 320, (2008).

Majimel J., Casanove M. J., Molénat G., «A 2xxx aluminum alloy crept at medium temperature: role of thermal activation on dislocation mechanisms”. *Materials Science and Engineering: A*, 380(1–2), p.110-116, (2004).

Nie J. F., Muddle B. C., “On the form of the age-hardening response in high strength aluminium alloys”. *Materials Science and Engineering A*, 319-321:448–451, (2001).

Rzyńska G., Gieleta R., “Experimental and numerical modeling of the extrusion process in 1050a aluminum alloy for design of impact energy-absorbing devices”, *Strength of Materials*, 48, 552-560, (2016).

Slotaj J., Diser M., “Advanced material models for stamping of AW 5754 aluminum alloy” *Strength of Materials*, 48, 487-494, (2016).

Voce E., “The relationship between stress and strain for homogeneous deformations”, *Journal of the Institute of Metals*, 74, 537-562, (1948).

Williams J.C., Starke E.A., “Progress in structural materials for aerospace systems”, *Acta Mater*, 51, 5775–5799, (2003).

Wilm A., 1911, “Recherche sur la métallurgie physique des alliages Aluminium – Magnésium”. *Métallurgie*, 8, 225–7, (1911).

Znaidi A., Daghfas O., Gahbiche A., Nasri R., “Identification strategy of anisotropic behavior laws: Application to thin sheets of A5”, *Journal of Theoretical and Applied Mechanics*, 54, 1147-1156, (2016).

## NOMENCLATURE

$\psi$  : angle between the loading direction and the rolling direction

$\epsilon_{xx}$  axial strains

$\epsilon_{yy}$ , transverse strain

$\epsilon_{zz}$  normal strain

$\sigma$  instantaneous stress

$\sigma_{eq}$  : Equivalent stress

$\mathbf{q}$  modified stress deviator tensor

$q_{k=1,2,3}$  are the eigenvalues of  $\mathbf{q}$

$\mathbf{A}$  fourth order tensor

$\sigma^D$ : the stress deviator tensor.

$\sigma_y(\epsilon^p)$  the scalar variable of isotropic hardening.

$\epsilon^p$  the equivalent plastic strain.

$\dot{\lambda}$  the plastic multiplier

$r_\psi$  the Lankford coefficient

$\dot{\epsilon}_{yy}$  the plastic strain rates in-plane

$\dot{\epsilon}_{zz}$  the plastic strain rates through the thickness